

SPATIALLY RESOLVED MEASUREMENTS OF THE OZONE PRODUCTION
IN A SILENT DISCHARGE IN PURE OXYGEN

J. Hackmann, M. Heise, J.H. Schäfer, J. Uhlenbusch, J. Urbanek
Physikalisches Institut II, Universität Düsseldorf
D-4000 Düsseldorf, FRG

ABSTRACT

Space resolved measurements of the ozone concentration in the discharge volume of an ac-silent discharge are reported. The diagnostic of the discharge was done by interferometry yielding the gas temperature, and by absorption measurements to determine the local ozone concentration. The measurements confirm numerical calculations solving a simplified set of rate equations.

1. INTRODUCTION

The kinetics of the ozone production in the silent discharge of ozonizers has been studied by many authors both numerically and experimentally (see e. g. /1-4/). For the understanding of elementary processes and the design of ozonizers it is of interest to observe the transient ozone formation and the evolution of discharge parameters in a gas cell as it travels through the discharge chamber. In this work spatially resolved photometric and interferometric diagnostic is applied to a test ozonizer operated under various discharge conditions.

2. EXPERIMENTAL SETUP

For quantitative spatially resolved measurements inside the discharge chamber of the ozonizer the following conditions must be fulfilled:

1. The oxygen flow through the chamber must be laminar to avoid turbulent mixing of the gas.
2. No by-passing of oxygen outside the electrode region should be allowed. Otherwise a comparison of the ozone concentration inside the chamber and the total oxygen production measured at the outlet of the ozonizer is not possible.
3. Care has to be paid to the fact that the ozone formed inside the discharge region diffuses to the outer layers. This leads to an enhancement of the effective absorption length if the observation windows are not mounted close enough to the discharge region. Ozone diffuses also opposite to the flow direction so that the gas entering the discharge contains already a certain amount of ozone.

To meet these requirements the ozonizer was designed as shown in fig. 1.

The upper electrode is connected to high voltage. The lower electrode is grounded and water cooled. The dielectric placed on the grounded electrode is a glass plate of 0.125 cm thickness. The gap distance between the two rectangular stainless steel electrodes is 0.2 cm. Quartz-windows for side on observation are mounted close to the electrode region. By this arrangement the electrodes and the windows form a flow channel of rectangular cross section (0.2 cm x 6 cm) and a length of 8 cm. A total length of 9 cm can be observed through the windows. The special design of the gas inlet provides laminar flow inside the flow channel.

2.1 Interferometry

Because of the relatively high refractive index of ozone ($n - 1 = 5.11 \cdot 10^{-4}$) at normal conditions interferometry is a sensitive diagnostic. The total refractive index of the gas inside the discharge is also affected by the oxygen and the temperature increase. For the total change of the refractive index due to ozone formation and temperature rise we arrive at

N_0 is the number density at $T = 0^\circ\text{C}$ and $p = 760$ Torr, T_i the initial temperature of the gas at the inlet. Knowing the number densities of oxygen and ozone the temperature rise can be calculated from the measured change of the total refractive index. The latter was measured by a conventional Mach-Zehnder interferometer illuminated by a He-Ne-laser. The fringe pattern was recorded by an optical multichannel analyzer.

2.2 Photometry

The local ozone concentration was measured using the optical arrangement shown in fig. 2. The radiation of a mercury lamp is splitted into two beams. One beam is focussed into the ozonizer, the second is monitored as a reference signal. Both beams are chopped with different frequencies and the intensities are measured by the same multiplier. The multiplier signal is fed into two lock-in-amplifiers connected to a ratiometer. The optical system has spatial resolution of about 0.1 cm. The processing by lock-in-amplifiers and ratiometer is insensitive against fluctuating light emission and stray light of the Hg-lamp. The position of the ozonizer was scanned using a stepping motor. At higher ozone concentrations it is favourable to measure the absorption not in the center of the absorption profile at 255 nm but in the wings of the profile. The selection of the spectral range was provided by a monochromator and interference filters.

3. CALCULATIONS

As shown by many authors (e.g. /1-3/) the formation of ozone in a silent discharge takes place on two different time scales. Reactions in which electron collisions are involved are very fast (30 ns) whilst atomic and molecular reactions are

characterised by much larger time constants in the order of usec at a pressure of 1 bar. For computation purposes this behaviour allows the process of ozone production during one discharge cycle to be split into two regimes. Shortly after break down atomic oxygen is produced by electronic dissociation of O_2 and O_3 . Ozone formation is neglected. In the second phase electronic processes are no longer taken into account and the reactions of the atomic oxygen are considered. This procedure simplifies the set of time dependent rate equations remarkably. The solutions display quite well the main features of the ozone generation. An example is plotted in fig. 3 where the calculated ozone production in dependence from the residence time in the discharge is compared to experimental data.

4. RESULTS

4.1 Spatial dependence of the temperature.

In fig. 4 the change of the total refractive index is plotted versus distance in flow direction. O_2 enters the discharge region at $x = 0$. The open circles represent the results from interferometric measurements. Calculating the refractive index change due to the ozone content of the gas alone using the measured ozone concentration the upper line is obtained. The difference between the two lines is attributed to the rise of the gas-temperature. The resulting local temperature change is plotted in fig. 5. Fig. 6 shows that the heating of the gas in the discharge is a linear function of the residence time obtained by dividing the distance by the flow velocity. The heating itself is rather moderate (only a few K per s in the parameter range studied in this experiment). However, as the rate of decomposing reactions increases with increasing temperature /5/ in the temperature range at which ozonizers are usually operated the discharge length should be adjusted to the flow velocity not to exceed residence times of say 10 s.

4.2 Local ozone generation

An example of the local concentration of ozone inside the discharge determined from absorption measurements is plotted in fig. 7 for three different discharge voltages. The bars indicate the values measured by conventional integral methods at the output of the ozonizer. Conversion of the local dependencies into functions of the residence time as plotted in fig. 8 shows only a weak influence of the flow velocity on the ozone concentration.

5. CONCLUSIONS

It has been demonstrated that interferometric and photometric methods are well suited for local measurements of gas temperature and ozone concentration inside the discharge chamber of an ozonizer. The results show that the residence time is the main parameter to determine the ozone generation at fixed ac frequency and electrical field strength. Experiments to apply the diagnostics to a broader parameter range are in preparation.

References

- /1/ B. Eliasson and U. Kogelschatz
Journal de Physique **40** C 7, 271 (1979)
- /2/ V.I. Gebalov, V.G. Samoilovitch and J.V. Filippov
Journal de Physique **40** C 7, 347 (1979)
- /3/ S. Yagi and M. Tanaka
J. Phys. D.: Appl. Phys. **12**, 1509 (1979)
- /4/ J. Salge and P. Braumann
ISPC - 4, Zürich (1979), Vol. 2, p. 735
- /5/ C.H. Bamford and C.F. Tipper
Comprehensive chemical kinetics, Vol. 4
London 1972

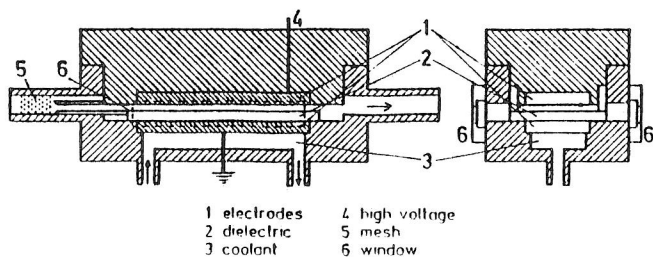


Fig. 1: Ozonizer for spatially resolved measurements

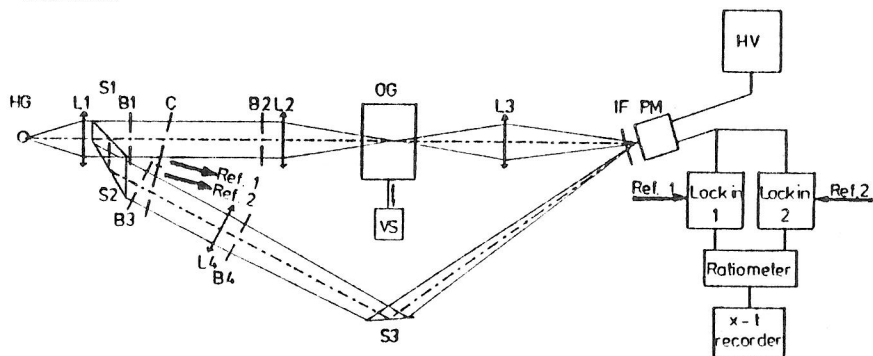


Fig. 2: Optical set up for photometry

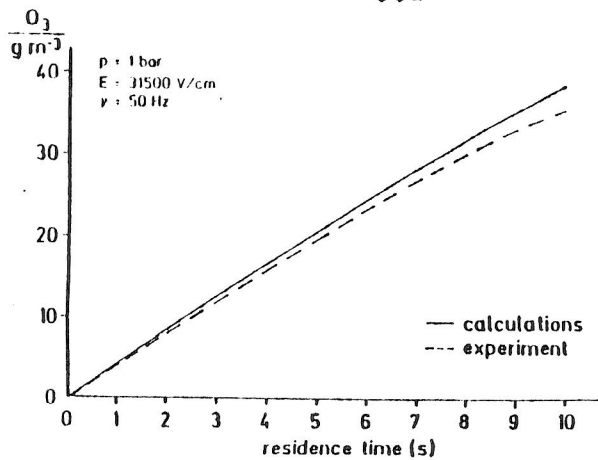


Fig.3: Ozone concentration as a function of residence time

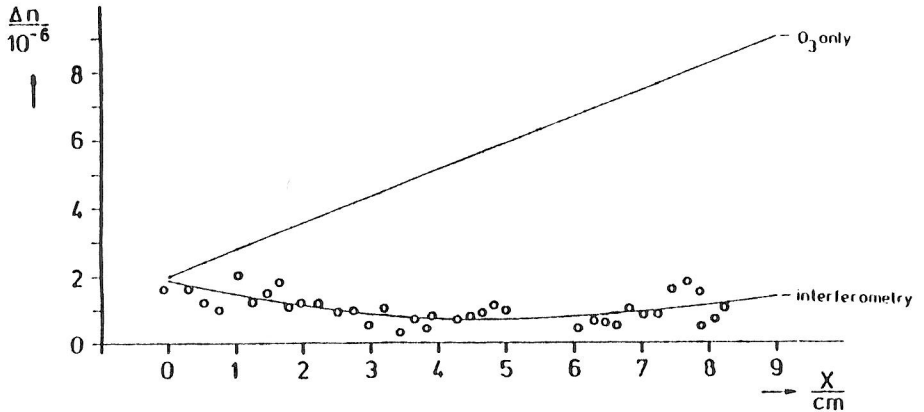


Fig.4: Local change of refractive index due to ozone generation and gas heating. Parameters: $p = 0.98\ bar$; $v = 1\ cm/s$; $\nu = 50\ Hz$; $E = 46.1\ kV/cm$

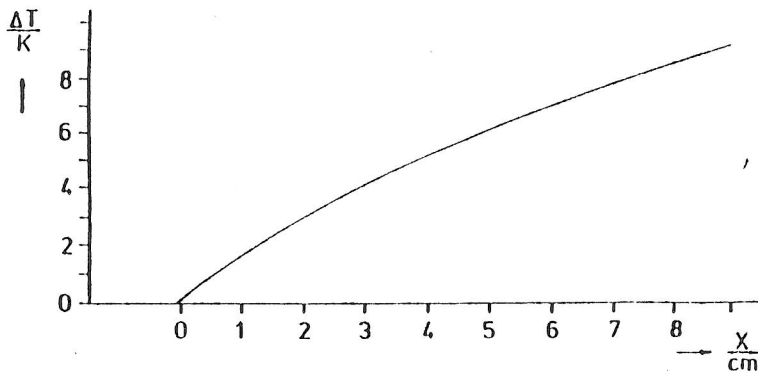


Fig.5: Local temperature rise as deduced from Fig.4.

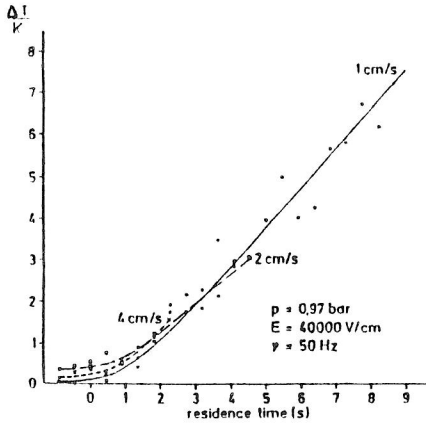


Fig. 6: Temperature rise as a function of residence time at various flow velocities

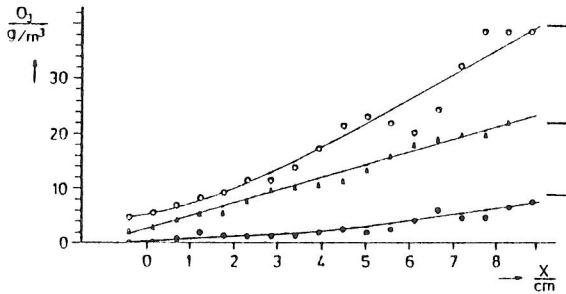


Fig. 7: local ozone concentration

$p = 0.98$ bar; $v = 2.2$ cm/s; $\gamma = 50$ Hz;

$E = 46.1$ kV/cm ○ ; $E = 39.9$ kV/cm ▲ ; $E = 27.6$ kV/cm ●

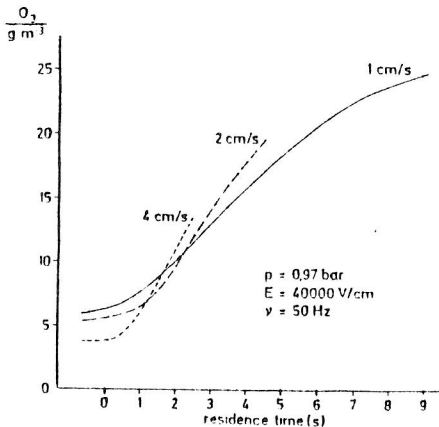


Fig. 8: Ozone concentration as a function of residence time